Differential Binding of L- vs. D-isomers of Cationic Antimicrobial Peptides to the Biofilm Exopolysaccharide Alginate

Lois M. Yin[a], Soyoung Lee[a], Jacky S.W. Mak[b], Amr S. Helmy[b] and Charles M. Deber*[a,c]

[a]*Division of Molecular Structure & Function, Research Institute, Hospital for Sick Children, Toronto M5G 1X8;* [b]*Department of Electrical and Computer Engineering, University of Toronto, Toronto M5S 3G4; and* [c]*Department of Biochemistry, University of Toronto, Toronto M5S 1A8, Ontario, Canada*

Abstract: Alginate is a biofilm exopolysaccharide secreted by the opportunistic pathogen *Pseudomonas aeruginosa* that acts to prevent the diffusion of antibiotics toward the bacterial cell membrane. Cationic antimicrobial peptides (CAPs) have been increasingly recognized as a viable alternative for prospective antimicrobial agents. The D-isomer chiral counterparts of active L-isomer CAPs tend to show slightly greater antimicrobial activities because bacteria lack proteases to hydrolyze the unnatural D-isomers. Using an enantiomeric pair of synthetic CAPs designed in our laboratory (L-4Leu in the sequence KKKKKKALFALWLAFLA–NH_2 and its D-analog D-4Leu), we studied the binding and interactions of L- vs. D-isomers of CAPs with alginate using circular dichroism and Raman spectroscopic techniques. We found that the peptide D-4Leu underwent a more rapid structural transition over time from an initial alginate-induced α-helical conformation to a less soluble β-sheet conformation than L-4Leu, indicating that the D-isomer of this peptide has a relatively greater affinity for alginate. Through Raman spectroscopy it was observed that Raman modes at 1297 cm^{-1} and 1453 cm^{-1} wavenumbers were found to differ between the spectra obtained from the insoluble complexes formed between L-4Leu vs. D-4Leu and alginate. These modes were tentatively assigned to CH, and CH_3 deformation modes, respectively. Our findings reveal previously undetected subtleties in the binding of this diastereomeric pair of peptides in the microenvironment of a biofilm exopolysaccharide, and provide guidelines for future development of antimicrobial peptides.

Keywords: Cationic antimicrobial peptides, alginate, biofilm, circular dichroism spectroscopy, Raman spectroscopy, peptide-exopolysaccharide complexes.

INTRODUCTION

Bacteria colonized into biofilms cause significant environmental and medical problems, including dental and medical device-related infections, infective endocarditis, and cystic fibrosis pneumonia [1-5]. Biofilm formation is characterized by the overproduction of exopolysaccharides, which act to curtail the diffusion of conventional antibiotics to the bacterial cell membrane [6-8]. There is accordingly an urgent need for new approaches to treat biofilm microbial infections.

Cationic antimicrobial peptides (CAPs) have become increasingly recognized as an alternative therapeutic approach to combat bacterial infections. CAPs are innate immunity agents that are highly selective against the bacterial membranes, as they bind to - and physically disrupt - the membranes of bacteria, leading to cell lysis and death [9]. In previous work, our laboratory has designed synthetic CAPs with the prototypic sequence KKKKKKAXFAXWXAFXA-NH_2[10,11], where X = various combinations of Ala or Leu residues; these CAPs exhibit excellent minimum inhibitory concentrations (MICs) against common bacteria such as *E. coli* and *P. aeruginosa*, and display little or no hemolysis against human erythrocytes. The D-chiral versions of active L-peptides have traditionally shown slightly greater activity [12,13], ostensibly because endogenous bacterial proteases are unable to hydrolyze the unnatural D-isomers [14]. And in fact, our MIC data have also shown that our designed D-CAPs are more effective than corresponding L-CAPs in killing multiple bacterial strains, including planktonic *Pseudomonas aeruginosa* [10, 15]. As well, Kolodkin-Gal *et al.* suggested that uptake by bacteria of certain D-amino acids (notably Trp and Tyr) may additionally act as delivery vectors that directly introduce selected D-amino acids to the detriment of the bacterial cell wall anchoring fibers and the disassembly of biofilm formation [16]. Amino acid residue chirality is thus an important factor contributing to effective CAP design.

However, little is known about whether there exists any difference in the physical interactions of L- vs. D-isomers of CAPs with biofilm exopolysaccharides. One of the most extensively studied biofilm exopolysaccharides is alginate from *P. aeruginosa* mucoid strains [17], which is an anionic heteropolymer consisting of β-(1-4)-D-mannuronate (M) and β-(1-4)-L-guluronate (G) monosaccharides[18], with each sugar containing a carboxylate group. Our lab has previously found that alginate competes with the similarly negatively-charged bacterial membrane by trapping the CAPs via charge neutralization and promoting peptide 'premature' conformational changes of the type normally associated with

*Address correspondence to this author at the Division of Molecular Structure & Function, Research Institute, Hospital for Sick Children, Toronto M5G 1X8; Tel: 416-813-5924; Fax: 416-813-5005;
E-mail: deber@sickkids.ca

1875-5305/13 $58.00+.00

CAP insertion into a membrane environment [19,20]; such a peptide-alginate complex is formed via electrostatic attraction followed by hydrophobic interaction between the two species [21]. Since the pyranosol rings of alginate have asymmetric faces, and peptides likely bind to alginate at preferential interaction sites, it is reasonable to hypothesize that the diastereomeric complexes formed between alginate and the L- vs. D-isomer of enantiomeric CAPs may differ in structural detail, and/or in the extent and affinity of peptide-polysaccharide association. To address this situation and guide further CAP design, we used circular dichroism and Raman spectroscopy techniques to compare the interactions between a representative pair of all-L and all-D synthetic CAP isomers of sequence KKKKKKALFALWLAFLA-NH_2 [10,11] and alginate.

MATERIALS AND METHODS

Peptide Synthesis and Purification

The L- and D-isomeric pair of the peptides with the sequence: KKKKKKALFALWLAFLA-NH_2 (termed L-4Leu and D-4Leu) were synthesized via continuous flow Fmoc solid-phase chemistry on a PS3 Protein Technologies Inc. synthesizer using a standard cycle [22]. Fmoc-PAL-polyethylene glycol-polystyrene resin (Applied Biosystems) was used to produce an amidated C-terminus on the final product. O-(7-azabenzotriazol-1-yl)-*N,N,N',N'*-tetramethyl-uroniumhexafluorophosphate (HATU) (GL Biochem (Shanghai) Ltd.) and *N,N*-diisopropylethylamine (DIEA) (Sigma-Aldrich) were used as the activation pair. Cleavage and deprotection of the peptides were performed in a mixture of 88% trifluoroacetic acid (TFA), 5% phenol, 5% water, and 2% triisopropylsilane (TIPS) for 2 hr in dark at room temperature. The crude peptides were purified by reverse-phase high performance liquid chromatography (RP-HPLC) on a C4 preparative column (Phenomenex) using a linear gradient of acetonitrile in 0.1% TFA. Peptide molecular weights were confirmed by mass spectrometry with expected (M+1) peaks. Peptide concentrations were determined using the micro BCA protein assay.

Alginate Purification

Alginate (Sigma-Aldrich) was purified as previously described [23]. Briefly, 1% alginate in 1 mM EDTA was precipitated by dropwise addition of 2 M HCl on ice until the pH reached 2.5, and washed with 0.01 M HCl containing 20 mM NaCl to remove the soluble impurities. The precipitated alginate was re-dissolved by bringing the pH up to 7.0 with dropwise addition of 0.5 M NaOH. Alginate was extracted twice in a chloroform/butanol mixture (4:1 v/v) to remove potential lipids and polyphenols [24]. The aqueous layer containing alginate was precipitated with 100% ethanol, washed with diethyl ether, and lyophilized overnight.

Circular Dichroism

Circular dichroism (CD) spectra were recorded on a Jasco-810 spectropolarimeter using a 1 mm path-length quartz cell at 25°C. CD experiments performed at various concentration ratios between the peptides and alginate (data not shown) indicated that samples using 20 μM peptide form the best initial helical structures in 0.1 mg/mL of alginate. Accordingly, 20 μM of each peptide was mixed with or without 0.1 mg/mL alginate in 20 mM Tris buffer, 10 mM NaCl, at pH 7.0. CD measurements were taken over a period of time each on an average of three scans with buffer background subtracted.

Raman Spectroscopy

Samples for Raman spectroscopy studies were prepared by adding 1 mM of the peptide of interest to 5 mg/mL of alginate solution. The resulting peptide-alginate precipitates were centrifuged for 5 min, separated from the supernatant, and dried by air. Raman spectra were measured using a Horiba Jobin Yvon LabRAM HR 800 spectrometer equipped with a continuous wave HeNe laser using 17 mW of power, 15 second exposure time, with averaging over 10 spectra. Background of the Raman spectra was removed through subtracting a 5-degree polynomial curve.

RESULTS

Secondary Structure of the Peptide L- vs. D-isomer Pair in Alginate Studied by Circular Dichroism

Both L-4Leu and D-4Leu peptides display a mixture of mainly random coil and partially α-helical structures in aqueous buffer (Fig. **1**, dashed lines). When each of the peptides was mixed with alginate (Fig. **1**, solid lines), there was an initial induction of α-helical conformation (two extrema at 208 and 222 nm). However, the peptides underwent a transition from the initial α-helical form to β-sheet structure (a single extremum at 216 nm) over an *ca.* 30 minute period in the presence of alginate. This phenomenon is presumably due to peptide-induced aggregation of the peptide-alginate

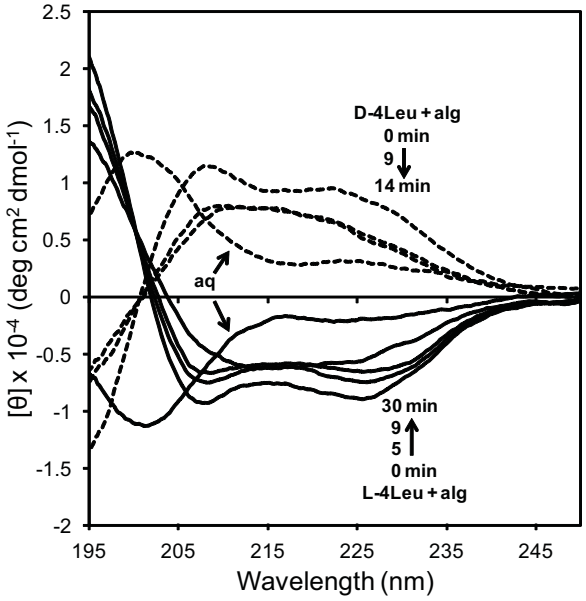

Figure 1. Time-dependent circular dichroism spectra of D-4Leu (dashed lines) and L-4Leu (solid lines) each in aqueous (aq) and in 0.1 mg/mL alginate solutions. The concentration of peptide is 20 μM in each experiment. Solutions are buffered at pH 7.0 in 20 mM Tris and 10 mM NaCl. Spectra are based on triplicate scans with buffer or alginate background subtracted.

complex [25], as fine solids eventually become visible in the sample cuvettes. The results suggest that there is a strong interaction between the CAPs and alginate that, at least with L-4Leu and D-4Leu CAPs, leads to the formation of largely insoluble peptide-alginate complexes.

Since the structural difference between the initial state (α-helix) and the final state (β-sheet) of each peptide is greatest at wavelength 206 nm, we compared the changes in ellipticity in CD spectra at 206 nm as a function of time (Fig. **2**). Importantly, we found that the half-life exponential decay time ($t_{1/2}$) as L-4Leu undergoes a loss of helicity is 15.57 ± 3.02 min, whereas the corresponding value for D-4Leu is 5.94 ± 1.08 min. These two $t_{1/2}$ values are significantly different ($p < 0.005$), confirming that the D-4Leu peptide forms peptide-alginate complexes significantly faster than the L-4Leu peptide, and indicating that peptide chirality plays a role in the kinetics of binding to alginate.

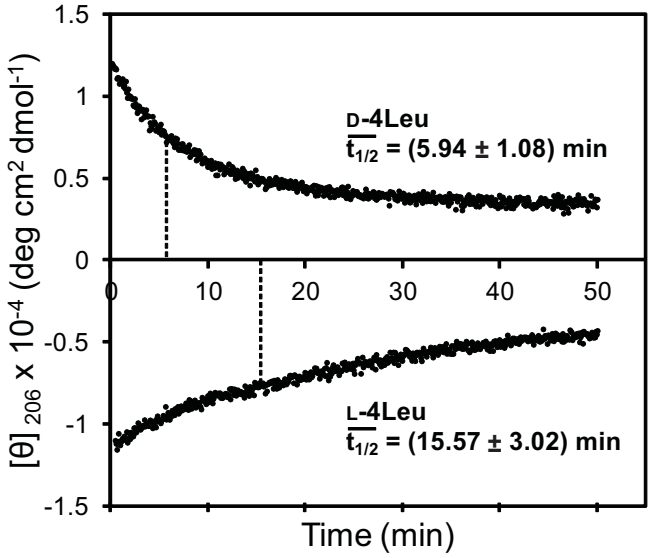

Figure 2. Changes in molar ellipticity at 206 nm of D-4Leu (top curve) and L-4Leu (bottom curve) as a function of time (min). The half-time decay constant (t1/2) value was estimated using an exponential decay function (GraphPad Prism), and averaged over 4 separate experiments for each peptide. Curves are shown for a typical experiment.

Peptide-alginate Complexes Studied by Raman Spectroscopy

To gain further insight into the nature of the specific interaction(s) – and any observable structural differences - with the peptide isomeric pair and alginate, Raman spectra were obtained from the L-4Leu peptide-alginate and D-4Leu peptide-alginate conjugates in solid form (Fig. **3**). We found that Raman modes of minor differential intensity were observed in the D-4Leu peptide-alginate spectra at 1297, 1483 and 1612 cm^{-1} that were absent in the L-4Leu peptide-alginate sample. These peaks were consistently observed in several replicates, indicating that the solid form of the sample has locked the final conformations of the peptide-alginate complexes. Such samples would correspond in principle to the endpoint peptide-alginate β-type states that appear in the CD experiments reported in (Figs. **1** and **2**).

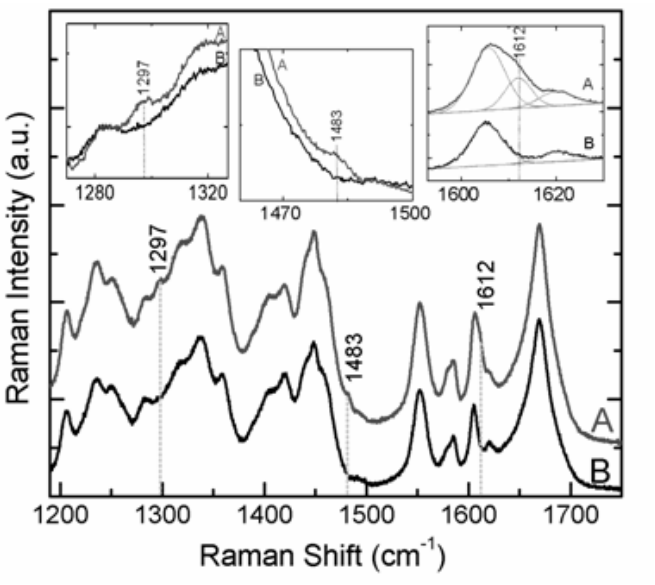

Figure 3. Raman spectra of (**A**) D-4Leu peptide – alginate; and (**B**) L-4Leu peptide – alginate complexes in the solid state. Spectra are offset vertically for clarity. Inset: Spectra expanded around Raman modes at 1297 cm-1 (left), 1483 cm-1 (middle), and 1612 cm-1 (right). Spectra in the 1612 cm-1 region are fitted with Gaussian functions as rendered in gray. Baselines are shown in gray below the curves. Spectra in the left and middle insets are overlapped to emphasize differences between curves.

In order to determine whether these Raman modes were correlated with varying interactions of the enantiomeric peptides with alginate, Raman spectra of the L-4Leu and D-4Leu peptides alone were each recorded. Fig. **4** shows the Raman spectra obtained from the two peptides in the regions where additional Raman modes were observed. The results indicate that the Raman mode at 1297 cm^{-1} was present in both the L-4Leu and D-4Leu peptide (Fig. **4A**) while the Raman mode at 1483 cm^{-1} was absent in both spectra (Fig. **4B**). However, the Raman mode at 1297 cm^{-1} was no longer detectable when L-4Leu interacted with alginate, while the mode at 1483 cm^{-1} emerged only when D-4Leu interacted with alginate.

Since the free L-4Leu and D-4Leu peptides are enantiomers, the fact that the Raman mode at 1612 cm^{-1} is observed in D-4Leu peptide but not in L-4Leu peptide (Fig. **4C**) suggests a role for sample history: given the tendency for either peptide to form β-structure in the presence of alginate (Fig. **1**), some minor self-aggregation of the D-peptide upon storage could similarly produce a measurable extent of β-aggregate, manifested by a Raman mode at 1612 cm^{-1}.

DISCUSSION

In the present study, we have investigated whether amino acid chirality affects the manner through which a cationic antimicrobial peptide binds to and interacts with the biofilm exopolysaccharide alginate. Using circular dichroism and Raman spectroscopy, we have compared the interactions between an enantiomeric pair of designed CAPs (L-4Leu vs. D-4Leu) and alginate.

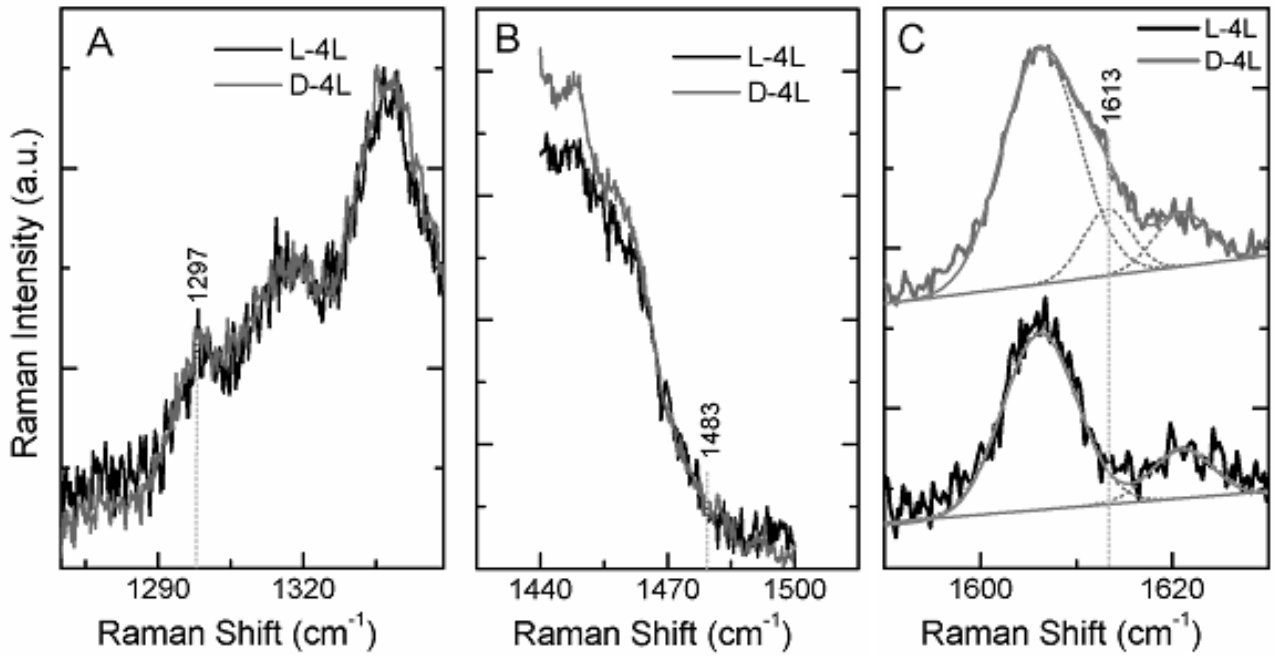

Figure 4. Raman spectra of D-4Leu (gray) and L-4Leu (black) peptides at shift regimes around (**A**) 1297; (**B**) 1483; and (**C**) 1612 cm-1. All spectra were normalized for comparisons. Spectra in (**A**) and (**B**) are overlapped to emphasize differences (if any) between curves; spectra in (**C**) are offset vertically for clarity, and fitted with Gaussian functions as rendered in gray dashed lines. Baselines are shown in gray below the curves.

CD experiments established that both L-4Leu and D-4Leu adopt α-helical conformations when they are first introduced to alginate, which supports the notion that alginate competes with bacterial membranes for binding accompanied by secondary structural induction for both L- and D-CAPs [19-21]. However, D-4Leu undergoes a more rapid transition than L-4Leu from the initial α-helical state to a β-sheet form of the peptide-alginate complex (Figs. **1** and **2**), suggesting that the D-4Leu has a greater tendency to bind to alginate than the L-4Leu. This finding parallels interactions of D- and L-enantiomers of poly-lysine and alginate analogs previously studied by Bystricky *et al.*, in which alginate rich in D-mannuronate strongly interacts with the D-isomer of poly-lysine but not significantly with its L-isomer, while alginate rich in L-guluronate weakly interacts with poly-D-lysine and not at all with poly-L-lysine [26]. Since our novel CAPs L-4Leu and D-4Leu also contain a (six-residue) poly-lysine motif, they may have a comparable interacting preference, *viz.*, both D-mannuronate and L-guluronate residues of alginate will interact more effectively with the D-form peptides than with the L-peptides. This phenomenon likely results from the complementary chiralities of the induced peptide conformation and the polysaccharide backbone. It is further noted that D-mannuronate residues of alginate form a three-fold left-handed helix [27,28]; such an asymmetric conformation may induce more effective complexation with D-peptides than with L-peptides [26]. On the other hand, L-guluronate residues of alginate form a rigid two-fold helix [29] that limits its interaction with both forms of peptides, a finding proposed to be due to incompatibility of charge densities [26].

The insoluble complexes formed between alginate and peptide isomers L-4Leu vs. D-4Leu were found to display differential Raman modes at 1297 and 1483 cm^{-1}. Although no conclusive assignments of these two modes could be made, tentative assignments can be proposed based on previously reported Raman literature values. For example, given that the 17-residue isomer pair of CAPs each contains mainly Ala and Leu residues in the hydrophobic core segment, the mode at 1297 cm^{-1} may be assigned to a CH deformation of the Leu side chain [30-32], while the mode at 1483 cm^{-1} may be assigned to a CH_3 deformation of the Ala side chain [32, 33].

Since the two peptides studied have identical sequences, the spectra of their alginate complexes would be expected to be largely comparable. Nevertheless, the overall results indicate that peptide isomers interact with alginate differently, *i.e.*, D-CAPs bind more tightly to alginate than L-CAPs. Once the cationic peptides have become bound to the anionic alginate via electrostatic attractions, both peptides eventually form insoluble complexes with the polysaccharide. The differential Raman modes (1297 and 1483 cm^{-1}) observed in the spectra of D-4Leu-alginate complex vs. L-4Leu-alginate complex support the suggestion that the interactions of Ala and/or Leu side chain CH and CH_3 substituents vary within the microenvironment of the alginate sugar rings.

CONCLUSION

The overall findings signal the relatively greater ability of the D-CAP to bind and crosslink/precipitate the anionic alginate - thereby disrupting the exopolysaccharide layer and potentially increasing the diffusion rate of additional free CAP molecules into and through the biofilm matrix to the bacterial membrane. These properties may be a useful consideration in the design of the most efficacious peptide antimicrobials.

CONFLICT OF INTEREST

The authors confirm that this article content has no conflict of interest.

ACKNOWLEDGEMENTS

This work was supported, in part, by a grant to C.M.D. from the Canadian Institutes of Health Research (CIHR FRN-79284), and to A.S.H from the Natural Sciences and Engineering Research Council (NSERC).

REFERENCES

[1] Hall-Stoodley, L.; Stoodley, P. Evolving concepts in biofilm infections. *Cell Microbiol.*, **2009**, *11*, 1034-43.

[2] Mohamed, J.A.; Huang, W.; Nallapareddy, S.R.; Teng, F.; Murray, B.E. Influence of origin of isolates, especially endocarditis isolates, and various genes on biofilm formation by *Enterococcus faecalis*. *Infect. Immun.*, **2004**, *72*, 3658-63.

[3] Lyczak, J.B.; Cannon, C.L.; Pier, G.B. Lung infections associated with cystic fibrosis. *Clin. Microbiol. Rev.*, **2002**, *15*, 194-222.

[4] Lee, B.; Schjerling, C.K.; Kirkby, N.; Hoffmann, N.; Borup, R.; Molin, S.; Hoiby, N.; Ciofu, O. Mucoid *Pseudomonas aeruginosa* isolates maintain the biofilm formation capacity and the gene expression profiles during the chronic lung infection of CF patients. *APMIS*, **2011**, *119*, 263-74.

[5] Wilson, A.; Gray, D.; Karakiozis, J.; Thomas, J. Advanced endotracheal tube biofilm stage, not duration of intubation, is related to pneumonia. *J. Trauma Acute Care Surg.*, **2012**, *72*, 916-23.

[6] Grobe, K.J.; Zahller, J.; Stewart, P.S. Role of dose concentration in biocide efficacy against *Pseudomonas aeruginosa* biofilms. *J. Ind. Microbiol. Biotechnol.*, **2002**, *29*, 10-5.

[7] Singh, R.; Ray, P.; Das, A.; Sharma, M. Penetration of antibiotics through *Staphylococcus aureus* and *Staphylococcus epidermidis* biofilms. *J. Antimicrob. Chemother.*, **2010**, *65*, 1955-8.

[8] Anderl, J.N.; Franklin, M.J.; Stewart, P.S. Role of antibiotic penetration limitation in *Klebsiella pneumoniae* biofilm resistance to ampicillin and ciprofloxacin. *Antimicrob. Agents Chemother.*, **2000**, *44*, 1818-24.

[9] Yeaman, M.R.; Yount, N.Y. Mechanisms of antimicrobial peptide action and resistance. *Pharmacol. Rev.*, **2003**, *55*, 27-55.

[10] Glukhov, E.; Burrows, L.L.; Deber, C.M. Membrane interactions of designed cationic antimicrobial peptides: the two thresholds. *Biopolymers*, **2008**, *89*, 360-71.

[11] Yin, L.M.; Edwards, M.A.; Li, J.; Yip, C.M.; Deber, C.M. Roles of hydrophobicity and charge distribution of cationic antimicrobial peptides in peptide-membrane interactions. *J. Biol. Chem.*, **2012**, *287*, 7738-45.

[12] Oren, Z.; Hong, J.; Shai, Y. A repertoire of novel antibacterial diastereomeric peptides with selective cytolytic activity. *J. Biol. Chem.*, **1997**, *272*, 14643-9.

[13] Huang, J.; Hao, D.; Chen, Y.; Xu, Y.; Tan, J.; Huang, Y.; Li, F. Inhibitory effects and mechanisms of physiological conditions on the activity of enantiomeric forms of an alpha-helical antibacterial peptide against bacteria. *Peptides*, **2011**, *32*, 1488-95.

[14] Blondelle, S.E.; Perez-Paya, E.; Houghten, R.A. Synthetic combinatorial libraries: novel discovery strategy for identification of antimicrobial agents. *Antimicrob. Agents Chemother.*, **1996**, *40*, 1067-71.

[15] Stark, M.; Liu, L.P.; Deber, C.M. Cationic hydrophobic peptides with antimicrobial activity. *Antimicrob. Agents Chemother.*, **2002**, *46*, 3585-90.

[16] Kolodkin-Gal, I.; Romero, D.; Cao, S.; Clardy, J.; Kolter, R.; Losick, R. D-amino acids trigger biofilm disassembly. *Science*, **2010**, *328*, 627-9.

[17] Flemming, H.C.; Wingender, J. The biofilm matrix. *Nat. Rev. Microbiol.*, **2010**, *8*, 623-33.

[18] Franklin, M.J.; Nivens, D.E.; Weadge, J.T.; Howell, P.L. Biosynthesis of the *Pseudomonas aeruginosa* extracellular polysaccharides, alginate, Pel, and Psl. *Front Microbiol.*, **2011**, *2*, 167.

[19] Chan, C.; Burrows, L.L.; Deber, C.M. Helix induction in antimicrobial peptides by alginate in biofilms. *J. Biol. Chem.*, **2004**, *279*, 38749-54.

[20] Chan, C.; Burrows, L.L.; Deber, C.M. Alginate as an auxiliary bacterial membrane: binding of membrane-active peptides by polysaccharides. *J. Pept. Res.*, **2005**, *65*, 343-51.

[21] Kuo, H.H.; Chan, C.; Burrows, L.L.; Deber, C.M. Hydrophobic interactions in complexes of antimicrobial peptides with bacterial polysaccharides. *Chem. Biol. Drug Des.*, **2007**, *69*, 405-12.

[22] Liu, L.P.; Deber, C.M. Anionic phospholipids modulate peptide insertion into membranes. *Biochemistry*, **1997**, *36*, 5476-82.

[23] De Vos, P.; De Haan, B.J.; Wolters, G.H.; Strubbe, J.H.; Van Schilfgaarde, R. Improved biocompatibility but limited graft survival after purification of alginate for microencapsulation of pancreatic islets. *Diabetologia*, **1997**, *40*, 262-70.

[24] Dusseault, J.; Tam, S.K.; Menard, M.; Polizu, S.; Jourdan, G.; Yahia, L.; Halle, J.P. Evaluation of alginate purification methods: effect on polyphenol, endotoxin, and protein contamination. *J. Biomed. Mater. Res. A*, **2006**, *76*, 243-51.

[25] Arutyunyan, A.M.; Rafikova, E.R.; Drachev, V.A.; Dobrov, E.N. Appearance of "beta-like" circular dichroism spectra on protein aggregation that is not accompanied by transition to beta-structure. *Biochemistry (Mosc)*, **2001**, *66*, 1378-80.

[26] Bystricky, S.; Malovikova, A.; Sticzay, T. Interaction of acidic polysaccharides with polylysine enantiomers - conformation probe in solution. *Carbohydr. Polym.*, **1991**, *15*, 299-308.

[27] Atkins, E.D.; Mackie, W.; Smolko, E.E. Crystalline structures of alginic acids. *Nature*, **1970**, *225*, 626-8.

[28] Atkins, E.D.T.; Isaac, D.H.; Nieduszynski, I.A.; Phelps, C.F.; Sheehan, J.K. The polyuronides: their molecular architecture. *Polymer*, **1974**, *15*, 263-271.

[29] Mackie, W.; Perez, S.; Rizzo, R.; Taravel, F.; Vignon, M. Aspects of the conformation of polyguluronate in the solid state and in solution. *Int. J. Biol. Macromol.*, **1983**, *5*, 329-341.

[30] Façanha Filho, P.F.; Freire, P.T.C.; Lima, K.C.V.; Mendes Filho, J.; Melo, F.E.A.; Pizani, P.S. High temperature Raman spectra of L-leucine crystals. *Braz. J. Phys.*, **2008**, *38*, 131-137.

[31] Bougeard, D. Phase Transition and vibrational spectra of I-Leucine. *Berichte der Bunsengesellschaft für physikalische Chemie*, **1983**, *87*, 279-283.

[32] Zhu, G.; Zhu, X.; Fan, Q.; Wan, X. Raman spectra of amino acids and their aqueous solutions. *Spectrochim. Acta A Mol. Biomol. Spectrosc.*, **2011**, *78*, 1187-1195.

[33] Lima, J.A.; Freire, P.T.C.; Melo, F.E.A.; Filho, J.M.; De Sousa, G.P.; Lima, R.J.C.; Façanha Filho, P.F.; Bordallo, H.N. Low-temperature Raman spectra of racemate DL-Alanine crystals. *J. Raman Spectrosc.*, **2010**, *41*, 808-813.

Received: December 20, 2012 Revised: February 22, 2013 Accepted: February 22, 2013